ADVANCED MATERIALS TECHNOLOGIES
www.advmattechnol.de

Microfluidically Produced Microcapsules with Amphiphilic Polymer Conetwork Shells

*Sara T. R. Velasquez, Andrea Belluati, Elena Tervoort, Iacopo Mattich, Brigitte Hertel, Sam Russell, Micael G. Gouveia, Patrick Grysan, Clément Mugemana, André R. Studart, and Nico Bruns**

Microcapsules with an aqueous core can be conveniently prepared by water-in-oil-in-water double emulsion microfluidics. However, conventional shell materials are based on hydrophobic polymers or colloidal particles. Thus, these microcapsules feature a hydrophobic shell impermeable to water-soluble compounds. Capsules with semipermeable hydrogel shells have been demonstrated but may exhibit poor mechanical properties. Here, amphiphilic polymer conetworks (APCNs) based on poly(2-hydroxyethyl acrylate)-*linked by*-polydimethylsiloxane (PHEA-*l*-PDMS) are introduced as a new class of wall materials in double emulsion microcapsules. These APCNs are mechanically robust silicone hydrogels that are swellable and permeable to water and are soft and elastic when dry or swollen. Therefore, the microcapsules can be dried and rehydrated multiple times or shrunken in sodium chloride salt solutions without getting damaged. Moreover, the APCNs are permeable for hydrophilic organic compounds and impermeable for macromolecules. Thus, they can be loaded with macromolecules or nanoparticles during microfluidic formation and with organic molecules after capsule synthesis. The microcapsules serve as microreactors for catalytically active platinum nanoparticles that decompose hydrogen peroxide. Finally, the surface of the APCN microcapsules can be selectively functionalized with a cholesterol-based linker. Concluding, APCN microcapsules could find applications for the controlled delivery of drugs, as microreactors for synthesis, or as scaffolds for synthetic cells.

1. Introduction

Microfluidic devices allow the preparation of water-in-oil-in-water (W/O/W) double emulsions with defined droplet sizes. In these double emulsions, an oil layer separates a water-filled compartment from the surrounding bulk water. If the oil layer contains compounds that can cure and solidify, the double emulsion droplet can be converted into a microcapsule in which a thin shell surrounds a liquid aqueous interior.[1–7] These microcapsules are useful for several applications, including drug or fragrance delivery,[1,6,8] cosmetics and food additives encapsulation,[1] as microreactors for enzymes,[9] or as a shell for artificial cells.[5,9] Double emulsion capsules have also been used to encapsulate nanoparticles, for instance, TiO_2 and ZnO nanoparticles, to create catalytic systems that can degrade organic pollutants.[10]

Shell materials of these microcapsules can be synthetic or natural polymers, or colloidal particles that stabilize the oil phase. These components or their precursors must be soluble in the oil phase,

S. T. R. Velasquez, A. Belluati, S. Russell, N. Bruns
Department of Chemistry
Technical University of Darmstadt
Peter-Grünberg-Straße 4, 64287 Darmstadt, Germany
E-mail: nico.bruns@tu-darmstadt.de

S. T. R. Velasquez, A. Belluati, S. Russell, M. G. Gouveia, N. Bruns
Department of Pure and Applied Chemistry
University of Strathclyde
Thomas Graham Building, 295 Cathedral Street, Glasgow G1 1XL, UK

The ORCID identification number(s) for the author(s) of this article can be found under https://doi.org/10.1002/admt.202400109

DOI: 10.1002/admt.202400109

S. T. R. Velasquez, S. Russell, M. G. Gouveia, A. R. Studart, N. Bruns
Swiss National Center of Competence in Research Bio-Inspired Materials
Fribourg Switzerland

E. Tervoort, I. Mattich, A. R. Studart
Complex Materials
Department of Materials
ETH Zürich
Vladimir-Prelog-Weg 5, Zürich 8093, Switzerland

B. Hertel
Department of Biology
Technical University of Darmstadt
Schnittspahnstraße 3, 64287 Darmstadt, Germany

P. Grysan, C. Mugemana
Materials Research and Technology
Luxembourg Institute of Science and Technology
5 Avenue des Hauts-Fourneaux, Esch-sur-Alzette L-4362, Luxembourg

C. Mugemana
Adolphe Merkle Institute
University of Fribourg
Chemin des Verdiers 4, Fribourg 1700, Switzerland

namely an organic solvent that is not miscible with water. Thus, they are usually hydrophobic polymers, hydrophobic monomers, hydrophobic colloidal particles, or mixtures thereof. As a result, double emulsion microcapsule walls are also hydrophobic and, therefore, impermeable for water or water-soluble compounds unless the capsule wall is micro- or nanoporous. However, a shell that is semipermeable for water-soluble compounds is essential for many applications. These include, for example, applications requiring the slow release of hydrophilic cargo from the inside of the capsules or the transport of water-soluble substrates to reach the catalysts within capsule microreactors. One possibility to create more polar shells is to use polymers that are soluble in water and in organic solvents, such as poly(ethylene glycol) (PEG). Indeed, hydrogel microcapsules could be prepared by polymerizing PEG macro crosslinkers, such as α,ω-dimethacrylate-terminated PEG.[9,11] However, when dried, PEG hydrogels lose their elasticity and, therefore, it is difficult to dry such hydrogel microcapsules without damaging the capsules. Other approaches to creating double emulsion microcapsules that allow for the transport of hydrophilic compounds across their shell have been proposed. For example, capsules with a permeable self-healing shell have been prepared using a dynamically crosslinked polymer network that can seal holes formed upon capsule cracking.[12] In other instances, permeable capsules have been made through phase separation of polymers during UV-induced polymerization of the middle oil fluid,[13] or by packing colloids in the middle phase to form colloidosomes with intrinsically microporous shells.[14] However, such microcapsules usually lack mechanical stability and toughness and may show limited functionalization capability.

Amphiphilic polymer conetworks (APCNs) can potentially address several of the drawbacks of currently available shell materials. APCNs are composed of chemically crosslinked hydrophilic and hydrophobic polymer chain segments and are exquisite materials with unique properties.[15–21] They are hydrogels that also swell in organic solvents. The materials undergo spinodal decomposition during polymerization.[22] However, the covalent crosslinks hinder macroscopic demixing of the chain segments of opposite polarity, so that the APCNs possess nanophase-separated morphologies that are often co-continuous over a broad range of compositions,[22–38] thereby allowing for diffusion of dissolved molecules across the material. This makes them semipermeable and suitable for membrane[39–44] and drug-delivery applications.[45–48] Moreover, they are transparent,[26,49–51] biocompatible,[48,52–57] and possess good mechanical properties, including elasticity when swollen and when dry,[26,37,55,58–63] lending themselves mechanically superior to other hydrogels. APCNs are used in everyday life as a material for extended-wear soft contact lenses,[64–67] and have been explored for drug delivery,[43,46,68–75] as biomaterials for the encapsulation of cells,[62,76,77] and for many other applications. Importantly, a common synthesis strategy toward APCNs is to copolymerize a hydrophobically masked monomer with a hydrophobic crosslinker, followed by conversion of the hydrophobic precursor network into an amphiphilic polymer conetwork by cleavage of the masking groups.[16,24,26,69,70,73,74] Thus, the monomer mixture is soluble in organic solvents and, therefore, fully compatible with the oil phase of microfluidics. Indeed, APCN microgel particles have been prepared by microfluidics.[73–75]

Here, we introduce APCNs as shell material for double emulsion-derived microcapsules. The type of APCN that we selected to prepare double emulsion microcapsules is poly(2-hydroxyethyl acrylate)-*linked by*-polydimethylsiloxane (PHEA-*l*-PDMS), a material which has been of long-standing research interest for our and other research groups. These APCNs are elastic materials,[63] and have been investigated for applications including semipermeable membranes,[26] as matrix for phase transfer reactions of enzymes in organic solvents[78,79] and supercritical CO_2,[80] as light-responsive membranes,[43] controlled release antimicrobial coatings,[81] as matrix for luminescent solar concentrators,[50,51,82] as material for colorimetric (bio)sensors,[83–85] and as self-sealing and puncture resistant breathable membranes.[86] Additionally, PHEA-*l*-PDMS APCNs can be functionalized post-polymerization by using the active ester pentafluorophenyl acrylate as an additional comonomer,[85,87] or they can be mechanically reinforced by the incorporation of peptide blocks between the PDMS segments and the crosslinking points.[63] Previously, PHEA-*l*-PDMS APCNs have been studied as a coating on surfaces,[26] as freestanding films and membranes,[26] as well as solid microparticles,[79] but not as capsules.

PHEA-*l*-PDMS microcapsules were prepared in a Lego-inspired microfluidic double emulsion device[88,89] and were loaded with platinum nanoparticles (PtNPs) as active catalysts during their microfluidic preparation. Inspired by the swelling and deswelling of pollen grains in response to various hydration levels,[90] the ability of capsules to recover after having been dried and rehydrated was studied. Moreover, the capsules' ability to osmotically shrink was examined by exposing them to high salt concentrations. The capsules are semipermeable for small water-soluble compounds but are impermeable for encapsulated macromolecules and colloids. This feature was harnessed to make microreactor capsules for the decomposition of hydrogen peroxide by the encapsulated PtNPs. Furthermore, the capsules' outer surface could be stably and selectively functionalized with a PEG_{3000}-cholesterol linker, whereby the cholesterol was inserted into the hydrophobic domains of the APCN.

2. Experimental Section

2.1. Materials

α,ω-methacryloxypropyl-terminated poly(dimethylsiloxane) (MA-PDMS-MA, viscosity 50–90 cSt, molecular weight = 4500–5500 g mol^{-1}) was purchased from ABCR (Germany). 2-Hydroxyethyl acrylate, triethylamine, chlorotrimethylsilane, photoinitiator bis(2,4,6-trimethylbenzoyl)-phenylphosphineoxide (Irgacure 819), poly(vinyl alcohol) (PVA; M_w 31 000–50 000, 87–89% hydrolyzed), dibenzocyclooctyne-Cy5 (Cy5-DBCO), 10-acetyl-3,7-dihydroxyphenoxazine (Amplex Red), Nile Red, 35% H_2O_2, FITC-Dextran (40 kDa), sodium fluorescein, myoglobin from equine heart and all inorganic salts for PBS and analytical grade solvents were purchased from Sigma–Aldrich. NanoXact Platinum Nanoparticles – Bare (Citrate) (5 nm, 0.05 mg mL^{-1} in aqueous 2 mM sodium citrate) (TEM Figure S7, Supporting Information) were bought from Biozol, Germany. Cholesterol-PEG_{3500}-azide was purchased from Broadpharmc (USA). All reagents were used as received unless otherwise stated.

2.2. Methods

2.2.1. Differential Scanning Calorimetry

Prior to analysis by DSC, all samples were dried overnight under vacuum at 50 °C. ≈10 mg of material was weighed into an aluminum DSC pan and sealed non-hermetically with an aluminum lid. The sample pan was then loaded into a Mettler Toledo DSC1. The sample and reference were heated from −150 to 150 °C at a scan rate of 10 °C $min^{-1,}$ and the resulting heat flow response was monitored. The sample was re-cooled to −150 °C and then reheated again to 150 °C, all at 10 °C min^{-1}. Nitrogen was used as the purge gas, at a flow rate of 150 mL min^{-1}. The glass transition temperatures were determined from the transition mid-points of the second heating curve.

2.2.2. Attenuated Total Reflection – Fourier Transform Infrared Spectroscopy

Prior to analysis by DSC, all samples were dried overnight under vacuum at 50 °C. The measurements were performed in a Bruker Alpha II FTIR in absorbance mode.

2.2.3. Thermogravimetric Analysis

Prior to analysis by TGA, all samples were dried overnight under vacuum at 50 °C. ≈10 mg of material was added into a pre-tared open aluminum pan and loaded into a Mettler Toledo TGA2. The sample was then heated at a rate of 10 °C min^{-1} from 25 to 350 °C, during which time the change in sample weight was recorded. Nitrogen was used as the sample purge gas, at a flow rate of 150 mL min^{-1}.

2.2.4. Light Microscopy

Microcapsules were imaged in transmission using a LEICA light microscope using LAS AF software, with magnifications of x5, x10, and x20. The samples were placed on glass slides for imaging.

2.2.5. Confocal Laser Scanning Microscopy

Confocal laser scanning microscopy was carried out using a Leica TSC SP8 confocal microscope equipped with an HC PL FLUOTAR 10x/0.30 DRY objective. For Nile Red labeling, 500 µL of capsules were mixed with 10 µL of a 1 mM solution of Nile Red in water without further purification. Afterward, 20 µL of MC suspension was placed in an 8-well chamber slide (Nunc Lab-Tek) with 200 µL of distilled water. When required, 10 µL of either fluorescein (2 mM) or FITC-Dextran 40 kDa (10 mg ml^{-1}) or 20 µL of Atto 488-labeled Mb (prepared according to previous protocols[91]) were added to the chamber slide. Imaging of the samples was performed by exciting each pixel line of the confocal scan sequentially (Fluorescein, FITC: ex. 488 nm, em. 505–525 nm; Nile Red: ex. 561 nm, em. 570–590 nm; Cy5: ex.635 nm, em. 660–690 nm). Time runs were acquired at 3 frames per minute, 580 s.

2.2.6. Scanning Electron Microscopy

Before SEM imaging, the samples were sputtered with a 6 nm layer of Pt using a CCU-010 (Compact Coating Unit), Safematic GmbH, CH. Scanning electron microscopy was carried out on a Leo 1530, Zeiss GmbH, Germany, using the secondary electron detector (SE detector) at an acceleration voltage of 3 kV.

2.2.7. Atomic Force Microscopy

Topography images and phase mode images were acquired in the air in tapping mode at scan rates of 1 to 3 Hz and a resolution of 512×512 pixels2 on an MFP3D INFINITY microscope (Oxford Instrument, UK). Semi-contact silicon AC160TS AFM tips (Olympus, Japan) with a cantilever spring constant of 26 N m^{-1} were used. Surface topography was acquired by maintaining the cantilever's first resonance amplitude constant via the feedback loop of the AFM acting on the piezo Z direction. The phase shift signal is recorded at the same time. Prior to the analysis, the APCNs were cleaned with water to remove residues that could compromise surface observation. To this end, a 100 µl aliquot of the APCN microcapsule suspension was added to 2 ml of deionized water in an Eppendorf tube. After shaking, the APCNs spheres were left to settle, and the supernatant was removed. The process was carried out a second time. The APCN microspheres were then transferred onto a cleaned stainless-steel plate and left to dry in the air. After taking the first set of AFM images, the microcapsules were rehydrated in water, dried again in air on the stainless-steel plate, and imaged a second time. Post-treatment of the topography raw data was done by removing a second-degree polynomial form via the software MountainSPIP (Digisurf, France).

2.3. Monomer Preparation

2.3.1. Synthesis of TMS-HEA

The TMS-HEA was prepared according to a previously reported procedure.[63]

2.4. Microcapsule Preparation

The microcapsules were prepared using a microfluidic three-way Lego-inspired device [88] connected to two individually controlled syringe pumps (Pump 33 DDS, Harvard Apparatus), one used for two syringes. Borosilicate round capillary tubes without filament were obtained from Sutter Instrument. Capillaries with an outer diameter of 2.00 mm and an inner diameter of 1.56 mm were used as outer capillaries. Tapered end inner capillaries were prepared by a micropipette puller from capillaries with an outer diameter of 1.00 mm and an inner diameter of 0.58 mm. The tapered end was grazed against abrasive paper to adjust the opening to the desired diameter, which was measured by optical light microscopy. The size of the capillaries was optimized. The inner capillary needed to have a diameter of 30–45 µm, with the collection capillary having a diameter of 100–150 µm of the inner capillary. The emitters were hydrophobized with a solution

of 5 wt% ODTMS, 0.5 wt%, n-butyl amine, and toluene. They were exposed for 4 h, then rinsed and dried.[92]

Experiments were carried out at room temperature in air, that is, without any measures to keep oxygen out of the system. The outer phase contained 2 wt% of PVA in MilliQ water. To this end, a stock solution of PVA was prepared by placing 10 wt% of PVA in MilliQ water at 80 °C overnight and further diluting with MilliQ water to 2 wt%. The middle phase contained a mixture of monomers to obtain PDMS-*l*-PHEA APCNs. 6150 mg (32.7 mmol) TMS-HEA were mixed with 3740 mg (0.374 mmol) MA-PDMS-MA, 660 µL of toluene, and 55 mg (1.31 mmol) photoinitiator. The inner phase contained either MilliQ water, 10 mg mL^{-1} FITC-Dextran 40 kDa in MilliQ water, or 1 wt% PtNP in MilliQ water. The outer phase had a speed of 50–80 mL h^{-1}, the middle phase 4–6 mL h^{-1}, and the inner phase 2.5–3 mL h^{-1}. The polymerization happened through the irradiation of the outflow before collecting them in a glass vial. The polymerization was done from the top using a UV–lab lamp with no filter, which was kept in a closed box while the capsules were collected in a glass vial. The irradiation was performed for 5 min during the collection. The capsules were collected in a glass vial, transferred into a 15 ml centrifugation flask, centrifuged at 4000 rpm (Centrifuge Z 306, Hermle Labortechnik GmbH), and resuspended in water. This process was repeated three times to remove PVA. Then, the capsules were left in a 1:1 isopropanol-water mixture, which was exchanged two times to cleave off the TMS groups from the polymer network and to remove toluene, yielding PHEA-*l*-PDMS APCNs with a 50:50 wt% composition of PHEA and PDMS, in analogy to the synthesis of PHEA-*l*-PDMS APCN films in the previous publications.[26,63,78] Some APCN capsules were further stained with Nile Red. To this end, 20 µL of the capsule suspension was added to 1 µL of 1 mM Nile Red in a vial and mixed in a vortex mixer for 90 s.

2.5. Microcapsule Dehydration/Rehydration Process

100 µL of the capsule suspension was placed on a glass slide in a vacuum oven for 30 min at 60 °C, 100 mbar. After removing the slide from the oven, the microcapsules were imaged as described in the main text. To rehydrate them, 100 µl MilliQ water was added to the capsules on the microscopy slide. The capsules were left at room temperature for 20 min before further characterization. The drying-rehydration cycle was repeated up to four times.

2.6. Microcapsule Shrinkage in NaCl Solution

The capsule shrinkage in brine was measured by adding 100 µL capsule suspension, the supernatant was removed, into 10 mL saturated NaCl solution in microscope slide wells and leaving the capsules submerged at room temperature until they stabilized (≈20 min). The capsules were imaged during this process by transmission light microscopy.

2.7. Determination of Microcapsule Concentration

10 µL of microcapsule suspension were placed on a glass slide and imaged on a Laborlux 12 ME ST (Leitz), equipped with a 10x objective. 3 different samples were counted (empty, with PtNP, and with FITC-Dextran), all yielding very similar results. The final concentration of microcapsules was calculated to be 2600 microcapsules mL^{-1}.

2.8. Fluorescein Release

2.8.1. Non-Dehydrated Capsules

20 µL of the NR-labeled microcapsule suspension were centrifuged (1 min, 2000 x g) and resuspended in a 1.5 mL Eppendorf centrifugation tube containing 1 mL of a 2 mM fluorescein solution in MilliQ water and incubated for 30 min at room temperature. During this time, fluorescein diffuses into the capsules so that they become loaded with the fluorescent dye. Afterward, the microcapsules were centrifuged (2000 x g). The supernatant was removed from the pellet, which was quickly (<10 s) washed to remove leftover unencapsulated fluorescein and then resuspended in 700 µL MilliQ water, incubating for 10 min to allow the diffusion of fluorescein to the outside. They were centrifuged again, and their supernatant was quickly transferred into a 96-well plate (triplicate wells per sample, 200 µL). Finally, the batches of pelleted capsules were resuspended in 700 µL water each, and the fluorescence of Nile Red was measured (triplicate wells per sample, 200 µL). A measurement of the ratio of fluorescein (ex. 495 nm, em. 505–525 nm) / Nile Red (ex. 561 nm, em. 570–590 nm) fluorescence (normalization of fluorescein signal against number of capsules, using the same pelleted capsules with their respective supernatant) was performed after 10 min on a Tecan Spark microplate reader. A scheme of the protocol is shown in Figure S7 (Supporting Information).

2.8.2. Dehydrated Capsules

1 mL of the NR-labeled microcapsule suspension was placed on a microscopy slide, and the capsules were dried at 60 °C, 100 mbar for 30 min in the vacuum oven. The dehydrated NR-labeled capsules were then rinsed from the microscopy slide into 1 mL MilliQ water, left to rehydrate (see above), then 20 µL were centrifuged again and resuspended in 1 mL of a 2 mM fluorescein solution in MilliQ water and incubated for 30 min at room temperature. The measurement proceeded in the same way as the non-dried capsules. The aliquot that was not incubated with fluorescein was dried and rehydrated again, up to 3 cycles.

2.9. Catalytic Activity

For each analysis, 10 µl of capsule suspension was added to wells in a 96-well plate. 5 µl of a 10 mg mL^{-1} Mb solution in PBS, 5 µL of a 0.3% H_2O_2 solution in water, 10 µL of a 100 µM Amplex Red solution in PBS (or equivalent PBS volumes) were added to each well, and the total volume was filled to 200 µL with PBS buffer. The different mixtures were incubated for 15 min at room temperature. The fluorescence emission measurements were performed using a Tecan Spark microplate reader (three wells per sample, excitation: 570 nm, emission 570–590 nm). To substitute the NP-loaded microcapsules with an equal amount of unencapsulated PtNPs, the total represented volume was calculated

by the lumen of the microcapsules. As it can be assumed that the final concentration of the inner aqueous phase, per capsule, is the same as the initial concentration, the total mass of encapsulated PtNPs present in the well was calculated by using their concentration and total volume in which they were distributed. Then substituted the microcapsules with free PtNPs and measured their activity.

2.10. Modification of the Capsule Surface with Cy5-PEG-Cholesterol

10 mg cholesterol-PEG_{3500}-azide was incubated with 12.11 mg Cy5-DBCO (final molar ratio 1:5) in 1 ml PBS for 1 h, then dialyzed overnight against 1 L PBS with a dialysis tube (regenerated cellulose, 1000 MWCO; Spectrapor, Spectrum), obtaining Cy5-PEG-cholesterol (CyPG). 10 µl of the CyPG solution was added to 50 µl of microcapsule suspension. Fluorescence measurements (ex. 645 nm, em. 660–690 nm) were performed immediately after adding the CyPG and after the capsules had been isolated by centrifugation (2000 x g) and resuspension in water, on a Tecan Spark microplate reader. The experiment was run in triplicates. Additionally, the capsules were imaged by CLSM to image the fluorophore distribution in the capsule wall.

3. Results and Discussion

The APCN double emulsion microcapsules were prepared using a Lego-inspired glass capillary microfluidic device developed by the group of Vladisavljević,[88,89] which offers a greatly simplified approach to double emulsion microfluidics compared to manually assembled glass capillary devices and allows the use of hydrophobic monomers. The device consists of two plastic blocks that can be easily joined together and separated using a Lego-inspired stud-and-hole coupling system that aligns the incorporated glass capillaries. The plastic blocks host two round glass capillaries inside a coaxially aligned round outer capillary.[88] **Figure 1** schematically shows the configuration of the capillaries and the overall experimental set-up for the preparation of double emulsion microcapsules. One syringe pump delivered, in two separate channels, the water-based inner phase and the middle oil phase, which contained toluene as water-immiscible solvent, as well as the hydrophobic monomer 2-(trimethylsilyloxy)ethyl acrylate (TMS-HEA), the hydrophobic macromolecular crosslinker a,w-dimethacrylate-terminated PDMS (MA-PDMS-MA) and a photoinitiator for free radical polymerization, in a 50:50 wt% composition of PHEA and PDMS. A second syringe pump delivered the 2 wt% of the PVA-based outer phase. W/O/W double emulsions were formed in the microcapillary device and collected in a vial, which was irradiated with UV light to initiate the polymerization and to form hydrophobic polymer conetworks in the oil phase. They were then converted into PHEA-*l*-PDMS amphiphilic polymer conetworks by cleaving the TMS groups in an isopropanol-water mixture.

The success of the double emulsification process and the size of the resulting APCN capsules depended on the diameters of the injection and collection capillary openings, the distance between the tip of the capillaries, and the flow rates of the three phases. The distance between the capillaries was 150 µm, and the diameter of the inner capillary and the collector were set to 100 and 350 µm, respectively. The flow rates were optimized for the given distance between capillaries to obtain double emulsion microcapsules, as examined by microscopy. The flow rate of the outer phase varied in the range of 50–80 mL h^{-1}, the flow rate of the middle phase varied between 4–6 mL h^{-1}, and the flow rate of the inner phase was set to values between 2.5–3 mL h^{-1}. It was not possible to form double emulsions if the inner capillary and collector were too close or if the speed of the middle and inner phases were in the same order of magnitude.

The microscopy image in Figure 1C shows an example of the capsules after the polymerization and TMS-cleavage step. In this typical batch, spherical APCN microcapsules with an outer diameter of 412 ± 23 µm and a shell thickness of 59 ± 14 µm were obtained when water-swollen. However, the capsule size could vary slightly with each batch. The shell of each capsule had a slightly asymmetric thickness, which is a commonly observed phenomenon for double emulsion microcapsules as the inner phase sinks within the oil phase shell before curing due to gravity, solvent evaporation, and the difference in flow speeds between the inner and middle phases.[93–95]

The shell of the capsules is optically transparent, which indicates that no macroscopic phase separation occurred during the synthesis of the APCNs, which would have resulted in turbid materials.[26] As PHEA and PDMS chain segments in the APCNs are not miscible, nanophase separation is expected to have occurred. The phase separation within the shell was confirmed by atomic force microscopy (AFM) and differential scanning calorimetry (DSC). In the phase mode AFM images, the PDMS domains appear dark and the PHEA domains appear bright.[26] The typical co-continuous morphology of APCNs can be observed, in which round, interconnected PDMS domains reside in a sponge-like PHEA matrix (**Figure 2**). Furthermore, there are some larger PHEA domains on the surface of the capsules, which indicates that a slight demixing at the surface occurred during capsule formation (Figure S1, Supporting Information). This is in accordance with previous observations made for PHEA-*l*-PDMS APCNs.[26] The morphology of the APCN microcapsules did not change significantly upon repeated rehydration and drying in water (Figure 2; Figure S1, Supporting Information). DSC of the APCN microcapsules revealed two glass transition temperatures at −123 °C, corresponding to PDMS,[96] and 4 °C, corresponding to PHEA [97,98] (Figure S2a, Supporting Information), which indicate polymer phase separation.

Thermogravimetric analysis under a nitrogen atmosphere indicated a mass loss with an onset at 150 °C and mass loss of 7% until 265 °C, after which the main mass loss proceeded over a relatively large temperature range up to 470 °C (Figure S2b, Supporting Information). The observed two-step mass loss corresponds most likely to the PHEA and PDMS chain segments of the APCN. Moreover, when PtNPs were present in the microcapsules, the mass loss in TGA experiments extended to above 550 °C. Attenuated total reflection Fourier-transform infrared (ATR FT-IR) spectra of dried APCN microcapsules show no evidence of the absorption bands at 1637 and 837 cm^{-1} (Figure S3, Supporting Information), indicating that the TMS group was cleaved off and that PHEA chain segments formed.

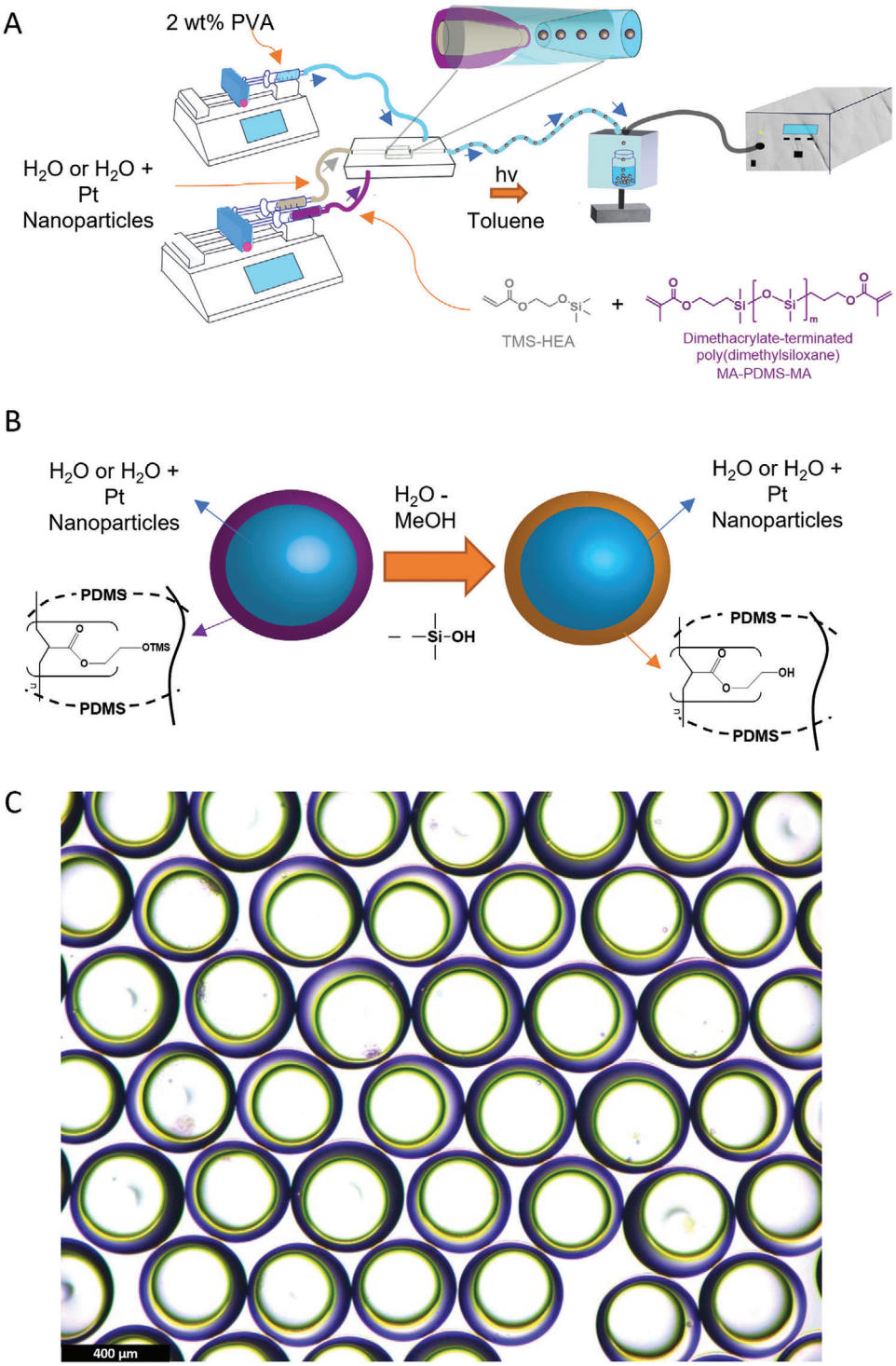

Figure 1. Schematic depiction of the Lego-inspired glass capillary microfluidic device and the experimental set-up used to produce double emulsion APCN microcapsules. A) Microfluidic formation of a double emulsion with a solution of monomer, macromolecular crosslinker, and photoinitiator in toluene as the oil middle phase, and an aqueous inner phase that optionally contained Pt nanoparticles, as well as an aqueous outer phase that contained polyvinyl alcohol (PVA) as surface active polymer. The double emulsion was irradiated with UV light to synthesize a hydrophobic polymer conetwork in the oil phase. B) Conversion of the hydrophobic precursor conetwork into a PHEA-l-PDMS APCN by cleavage of the TMS groups in a water-isopropanol mixture. C) Optical microscope image of APCN double emulsion microcapsules suspended in water. (The depicted microcapsules were prepared with PtNPs in the inner phase.) Scale bar: 400 µm.

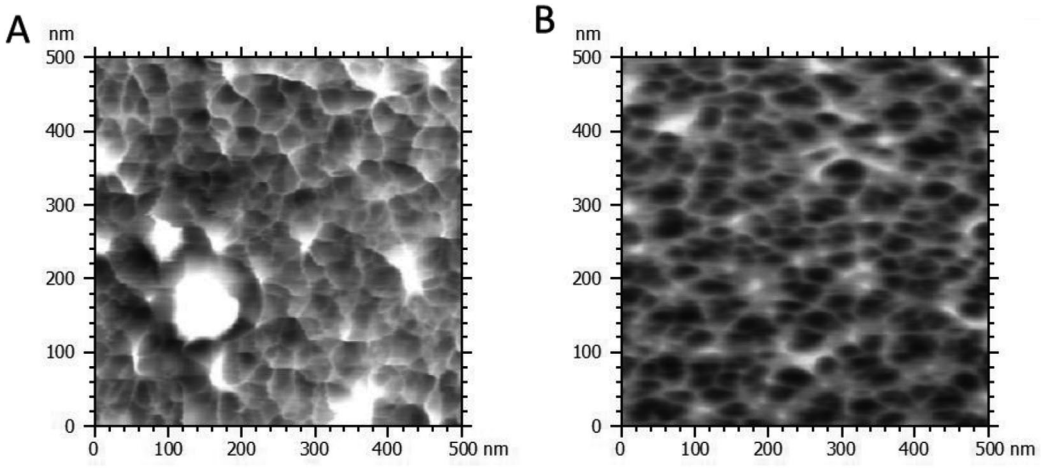

Figure 2. AFM phase mode images of the surface of dry APCN capsules loaded with PtNPs in the inner phase. A) First drying cycle. B) Second drying cycle.

Inspired by the dehydration and hydration of pollen grains, the drying and subsequent recovery of the microcapsules in water were studied through different drying-swelling cycles. One advantage of PHEA-*l*-PDMS over other microcapsule wall materials is that the APCNs are soft and flexible in both the swollen and dry states. **Figure 3** shows microscopy images of the capsules before, during, and after completing four drying-wetting cycles with water. The experiment reveals that the APCN microcapsules exhibit remarkable robustness even under the high stresses developed in the drying and rehydration processes. In the fully hydrated state, the capsules had a diameter of 266 ± 11 µm (Table S1, Supporting Information). When dried, they became deflated and bowl-shaped, most likely because the inner cavity of the capsules dried up and the capsule wall bulged inwards. After incubation in water for 20 min, the capsules recovered to a full spherical shape of the same size as before drying (Table S1, Supporting Information). This process could be repeated at least four times. No damage to the capsules was visible after each dehydration-rehydration cycle, indicating good recovery of the swollen APCN capsules, most likely because of the elastic nature of the capsule shell. In the microscopy images, the dry capsules seem to have cracks on their surface. However, scanning electron microscopy (SEM) images (**Figure 4**; Figure S4, Supporting Information) show that they are just wrinkles generated during drying. In the SEM images, the surface of the dry capsules after each of the drying steps appears smooth without any cracks or other defects, and the bowl-shape of the deflated capsules can be seen. This confirms that the capsules remained intact during the drying process and that the water inside of the capsules had left them by diffusing through the capsule wall.

Confocal laser scanning microscopy (CLSM) was used to quantify the thickness of the capsule wall (Figure S5, Supporting

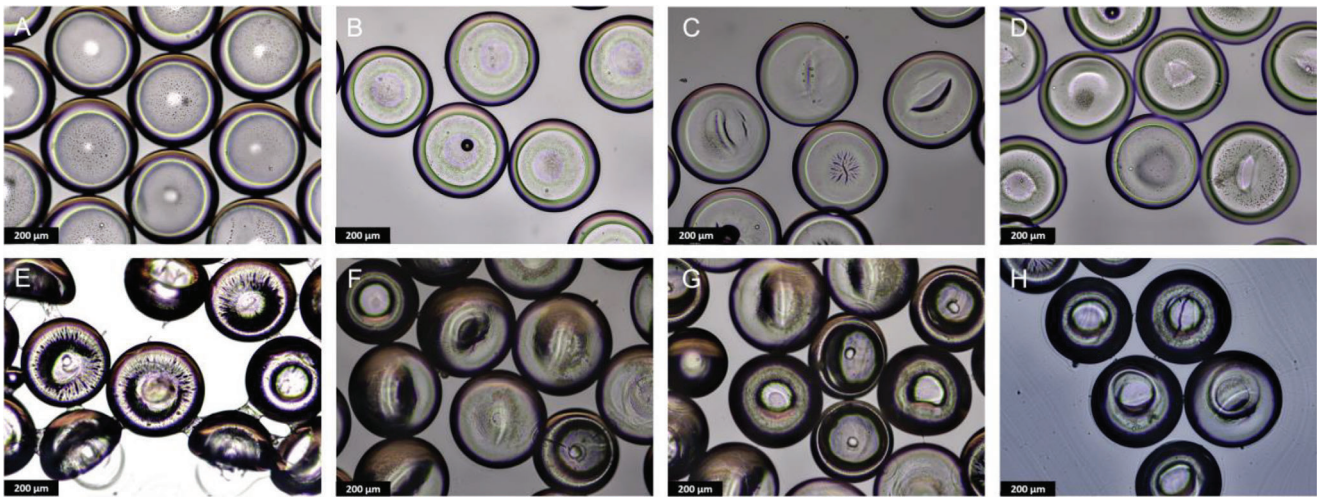

Figure 3. Transmission light microscopy images of hydrated and dry APCN microcapsules over 4 hydration and dehydration cycles. A–D) Hydrated microcapsules in water: A) As prepared, B) After the first dehydration-rehydration cycle, C) After the second dehydration-rehydration cycle, D) After the third dehydration-rehydration cycle. E–H) Dry microcapsules in air: E) After first dehydration, F) After second dehydration, G) After third dehydration, H) After fourth dehydration. The depicted microcapsules were prepared with PtNPs in the inner phase. Scale bars = 200 µm.

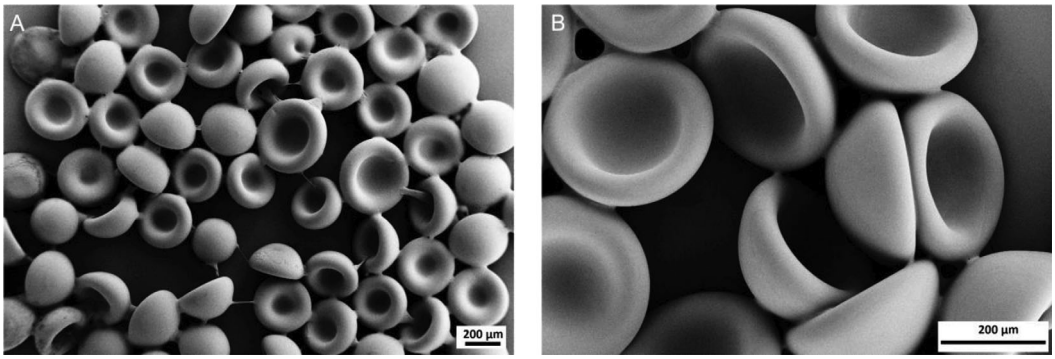

Figure 4. SEM images of dry APCN microcapsules after first dehydration. A) 100 x magnification. B) 300 x magnification. The depicted microcapsules were prepared with PtNPs in the inner phase. Scale bars = 200 µm.

Information). To this end, the capsules were fluorescently stained with Nile Red (NR) to highlight their polymeric shell. When hydrated, the capsule wall was 25–30 µm thick. When the capsules were dried, they adopted a bowl-like shape, which made an exact measurement of wall thickness difficult. Apparently, the thickness of the capsule wall increased to 55–85 µm, which corresponds to approx. two times the wall thickness, which would be expected when the shell bulges. Figure S5d–f (Supporting Information) shows the dry capsules after different numbers of dehydration-rehydration cycles. No cracks or other damage to the shell were observed, confirming the remarkable robustness and mechanical resilience of the APCN capsules.

Hydrated APCN microcapsules shrank when placed in a saturated salt solution, such as brine (**Figure 5**), most likely because the water diffused out of the capsules in response to the osmotic pressure across the capsule wall. The shrinking process took ≈20 min until the size of the capsules stabilized, with the capsule diameter decreasing from 263 ± 32 to 172 ± 40 µm. Moreover, shrinkage changed the shape of the capsules from spherical to bowl-like morphology.

The permeability of the microcapsule shell was studied using fluorescent dyes of different sizes (**Figure 6**; Figure S6; Video S1, Supporting Information). A small molecule like fluorescein (340 Da) could diffuse into the capsules, as shown Figure 6A and Video S1 (Supporting Information). However, Atto 488-labeled myoglobin (17 kDa) or FITC-labeled dextran (40 kDa) did not diffuse into the cavity (Figure 6B,C). Similarly, when FITC-labeled dextran was encapsulated in the inner cavity during capsule formation, the macromolecular cargo did not diffuse out of the capsules (Figure 6D). Thus, small molecules such as fluorescein permeated through the APCN capsule wall, while the APCN was impermeable to macromolecules such as myoglobin and dextran. As 40 kDa dextran has a radius of 4.5 nm,[99] the microcapsules should likewise retain similarly-sized colloids.

The influence of dehydration-rehydration cycles on the permeability of the microcapsule shell was studied with encapsulated fluorescein as a model compound. NR-labeled empty capsules were incubated for 30 min in a fluorescein solution to load them with the fluorescent dye, then centrifuged, quickly washed, and resuspended in water. Encapsulated fluorescein was then allowed to diffuse out of the capsules for 10 min. The capsules were sedimented by mild centrifugation, the supernatant was collected, and its fluorescence was measured. To normalize the fluorescence of released fluorescein to the concentration of capsules in the sample, the microcapsules were resuspended in water and collected to measure their NR fluorescence (**Figure 7**, Entry: 0 Rehydration cycles; Figure S7, Supporting Information). The same

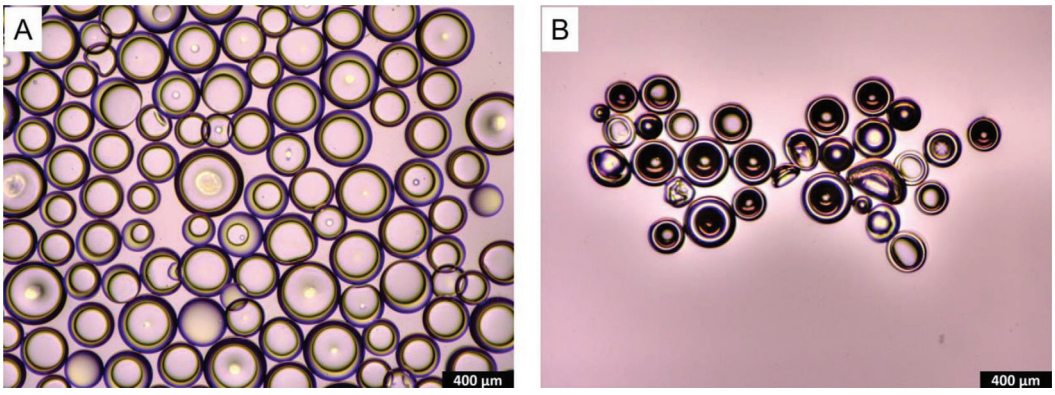

Figure 5. Shrinking of APCN microcapsules in saturated sodium chloride solution as observed by light microscopy. A) Capsules in water before the addition of brine. B) Capsules after 20 min in a brine solution. The depicted microcapsules were prepared with PtNPs in the inner phase. Scale bars = 400 µm.

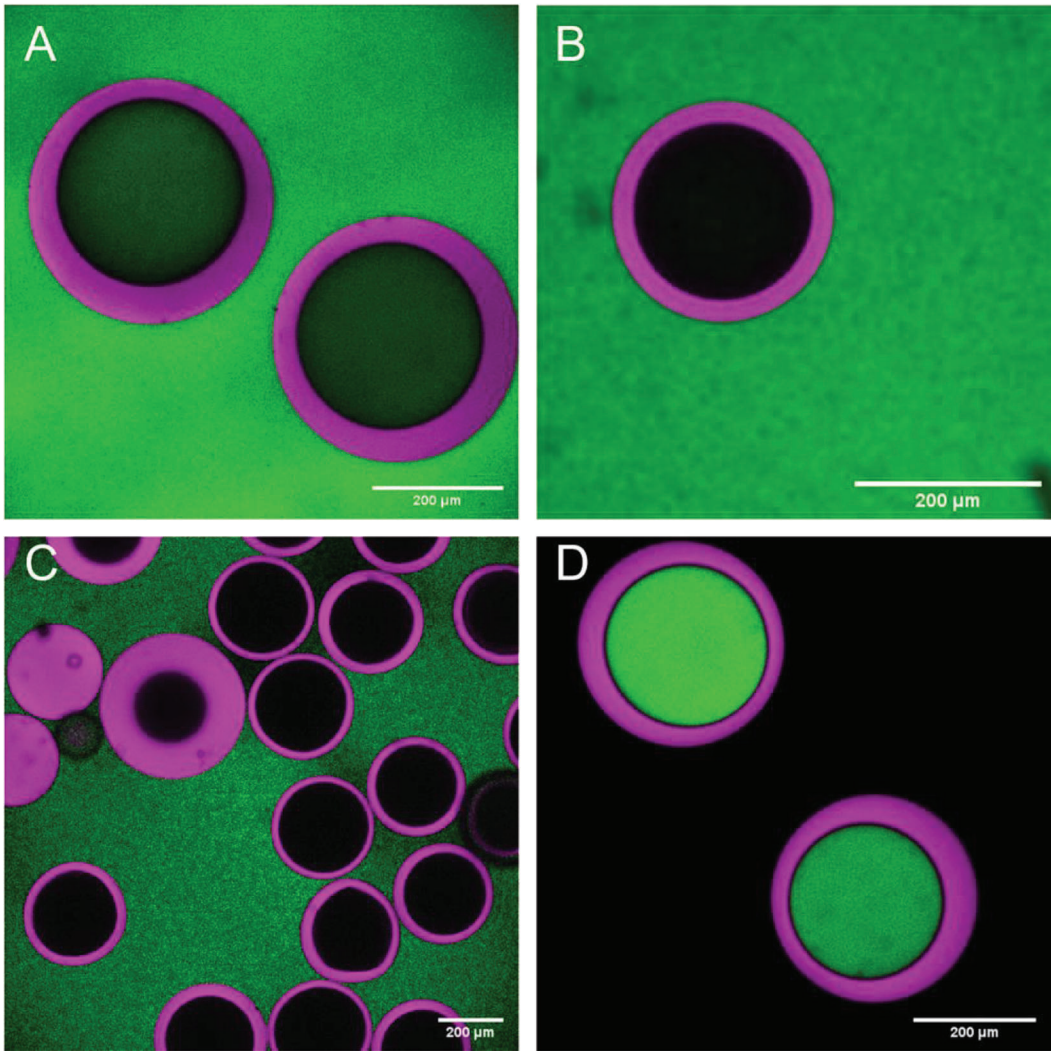

Figure 6. CLSM micrographs to assess the permeability of APCN microcapsules for fluorescein and impermeability for macromolecules. A) Nile Red-stained (magenta) microcapsules with fluorescein (green, 340 Da) that has diffused from the outside to the inner cavity, 30 min after addition of the microcapsules into a fluorescein solution. B) Nile Red-stained microcapsules with Atto 488-labeled myoglobin outside of the capsules, showing that myoglobin did not diffuse into the capsules. C) Nile Red-stained microcapsules with FITC-dextran (40 kDa) outside of the capsules after 30 min incubation, showing that FITC-dextran does not diffuse into the capsules. D) Nile Red-stained microcapsules loaded with FITC-Dextran 40 kDa during microfluidic double emulsion capsule preparation, showing that FITC-dextran was retained in the capsules. Scale bars = 200 µm. (The depicted microcapsules in A–C were prepared with PtNPs in the inner phase. The solid particles in C are either out-of-focus microcapsules or single emulsion microparticles that formed when one of the fluid phases was empty during microfluidic emulsification.) Scale bars = 200 µm.

fluorescein uptake and release procedure was carried out with APCN microcapsules that had been dried and rehydrated for one or more cycles (Figure 7). The experimental results show that dried and rehydrated microcapsules released more fluorescein than the never-dried ones. However, the release did not increase with increasing number of drying-rehydration cycles. As it can be assumed that the amount of fluorescein released after a fixed amount of time is proportional to the permeability of the shell, the results suggest that the permeability increased once upon drying and rehydration and remained constant in the subsequent cycles. Two possibilities could account for these results. Either the first drying induced small defects in the capsule shell that do not enlarge or increase in number in further drying events. However, such defects are not observed in the SEM images of the capsules, and it is also unlikely that additional drying steps would not damage the shell further. Alternatively, the arrangement of the hydrophilic PHEA and the hydrophobic PDMS in the APCN might change upon the first drying and rehydration step. Small changes in the connectivity between domains can greatly influence permeability, as demonstrated for silicone hydrogels.[100] Moreover there can be thin interfacial region between hydrophilic and hydrophobic domains that differs in their solvent content [30] or that shows a composition gradient.[100] Drying and rehydration forces the hydrophobic polymer chain segments to rearrange, which could possibly lead to a better connection between the hydrophilic domains, thereby making it easier

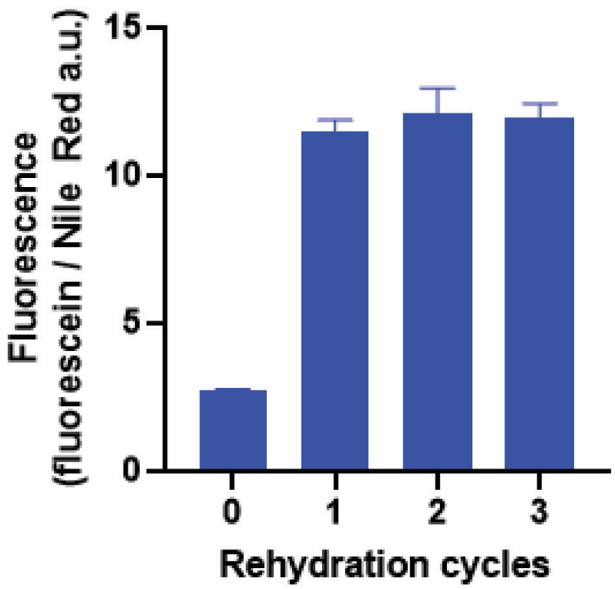

Figure 7. Release of fluorescein from APCN microcapsules over several dehydration-rehydration cycles. The capsules were stained with Nile Red, and the fluorescence of fluorescein in the surrounding liquid was normalized over Nile Red fluorescence, which is directly proportional to the concentration of capsules. Data shown as mean of n = 3 measurements ± S.D.

for the water-dissolved fluorescein to diffuse through the water-swollen microcapsule shell. The subsequent drying step did not change the morphology of the APCNs (Figure 2). Thus, the capability to release fluorescein remained constant.

One possible application of APCN microcapsules is as microcompartments for chemical reactions.[101] To explore this potential application, the capsules were loaded with platinum nanoparticles (PtNPs) that are catalysts, for example, for the decomposition of hydrogen peroxide into oxygen and water.[102] PtNPs were added to the inner aqueous phase during capsule formation by microfluidic double emulsification. The catalytic activity of the PtNP-containing APCN microcapsules was measured indirectly by a competition assay with myoglobin (Mb) that acts as a peroxidase [103,104] and that was added to the outside of the capsules (**Figure** 8A). Mb uses hydrogen peroxide to oxidize Amplex Red (AR) to the fluorescent resorufin. The presence of Mb in the suspension of NP-loaded capsules meant that H_2O_2 would be either used to oxidize AR or decomposed by the PtNPs without production of fluorescence.[105,106] The NP-loaded capsules partially quenched the activity of myoglobin (Figure 8B), indicating that the PtNPs decomposed hydrogen peroxide. Interestingly, this happened even though the enzyme had easier access to the substrates because hydrogen peroxide did not have to cross a polymer shell before reaching the enzyme.[107] In the absence of Mb, the catalyst-loaded capsules were even able to counteract the non-catalyzed oxidation of AR with H_2O_2.[99] Overall, it can be concluded that H_2O_2 can diffuse through the shell of the microcapsules and that the PtNPs inside of the APCN microcapsules are catalytically active in decomposing H_2O_2. This demonstrates that the capsules act as microreactors for the nanoparticles. As expected, however, the diffusion of substrates did play a role: when the microcapsules were substituted with unencapsulated PtNPs, at the same concentration, the activity of Mb was almost fully quenched, thus indicating that mass transfer is a limiting factor on the overall activity of the microreactors.[108]

While some molecules like fluorescein and hydrogen peroxide diffuse through the microcapsule shell and others, such as the lipophilic dye Nile Red, homogeneously distribute throughout the whole thickness of the APCN wall, the outside of the shell might be selectively functionalized with a hydrophobic moiety attached to a hydrophilic macromolecule. The hydrophobic moiety should act as an anchor that enters into the hydrophobic domains on the surface of the APCN, while the hydrophilic macromolecule hinders deep penetration into the APCN due to its bulkiness. To illustrate such a functionalization strategy, APCN microcapsules were incubated in a Cy5-PEG3500-cholesterol (CyPC) solution. This molecule contains a hydrophobic cholesterol anchor that is usually used for insertion into lipid and block copolymer membranes. The PEG is hydrophilic and acts as a spacer to ensure water solubility, and the Cy5 is a fluorescent moiety.

After incubation of APCN microcapsules in a solution of CyPC and subsequent purification of the capsules, the microcapsules remained fluorescent. This indicates that CyPC was retained after centrifugation, washing in water, and resuspension of the capsules in water (**Figure** 9A). CLSM micrographs show that the fluorescence was localized on the outside of the APCN shell (Figure 9B). Thus, CyPC did not diffuse through the whole membrane but selectively stained a thin outer layer of the capsule wall. The selective modification of the capsule surface with PEG-cholesterol should also allow the outer surface of the capsules to be decorated with other useful moieties, for example, functional groups for click chemistry to attach biomolecules.[91,109,110]

4. Conclusion

Mechanically robust microcapsules with water-swellable and semi-permeable shells can be prepared by microfluidic double emulsification using PHEA-*l*-PDMS APCNs as wall materials. By polymerizing a hydrophobically masked monomer with a PDMS-based macromolecular crosslinker, it became possible to create silicone hydrogels that are templated by the oil phase of the double emulsion and, therefore, form the shell of the microcapsules. These APCNs greatly expand the material scope of double emulsion microcapsules. For example, the APCN microcapsules can be dried and rehydrated multiple times without damage. They are semipermeable for water and small water-soluble compounds while retaining macromolecules on their inside. Moreover, they can host catalytically active nanoparticles and thereby serve as microreactors or be selectively modified with a suitable linker on their surface. Thus, APCN microcapsules should be useful for a variety of applications that involve encapsulation and controlled release of active compounds such as drugs or fragrances. Alternatively, they could be used as catalytically active building blocks for molecular systems engineering or as compartments for the preparation of artificial cells. Furthermore, APCNs are transparent, so that the capsules could also be used as adaptable optical materials such as microlenses.

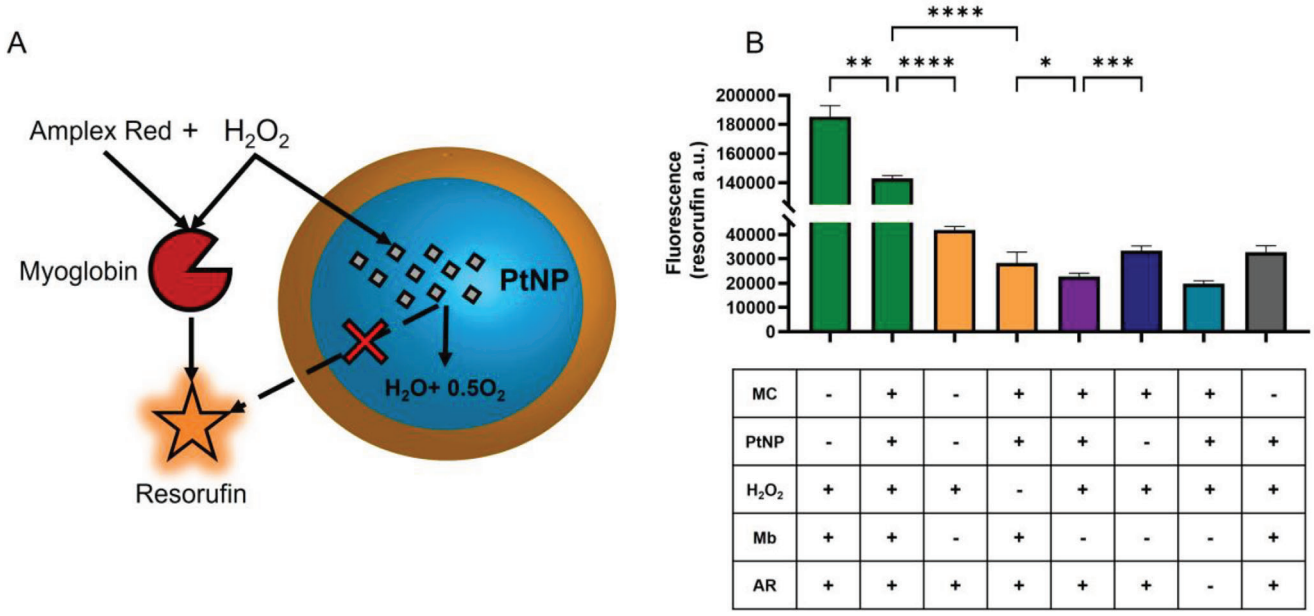

Figure 8. PtNP-loaded APCN microcapsules as microreactors for the catalytic decomposition of H_2O_2. A) Schematic depiction of the activity assay. To assess the H_2O_2 degradation, a competitive fluorometric assay was carried out in which myoglobin catalyzes the conversion of Amplex Red into resorufin under the consumption of H_2O_2. B) Results of the H_2O_2 decomposition assay. Microcapsules loaded with PtNPs (MC-Pt) and microcapsules without PtNPs (empty MC) in the presence and absence of Mb on the outside of the capsules, as well as several control reactions. The AR-less condition acts as negative control and shows the background fluorescence of the assay. Values as mean ± SD, n = 3. $^{*}p<0.05$, $^{***}p<0.001$, $^{****}p<0.0001$.

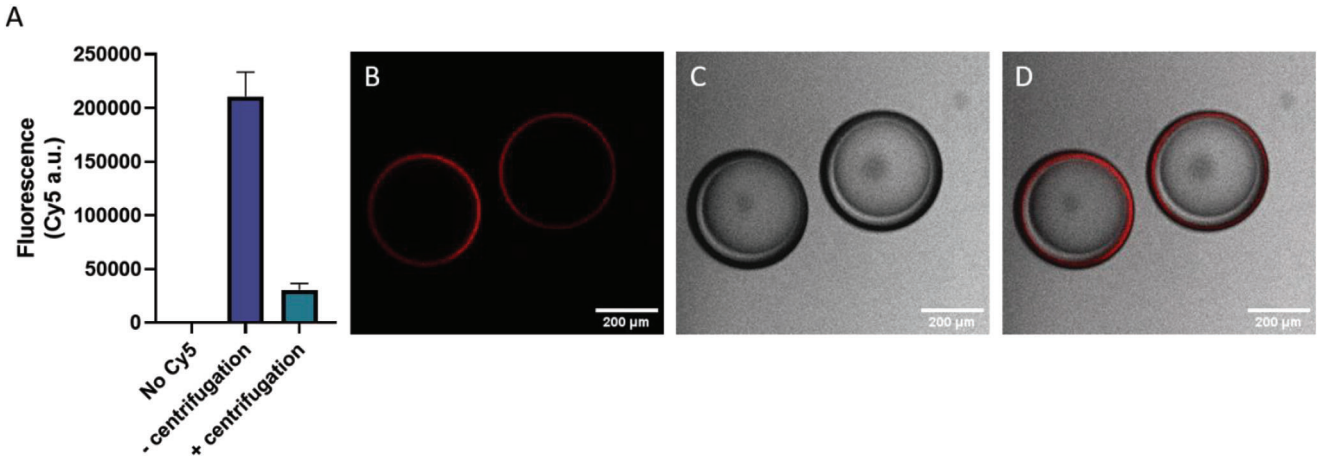

Figure 9. Surface functionalization of APCN microcapsules with Cy5-PEG_{3500}-cholesterol. A) Graph showing the fluorescence emission (660–690 nm) of the capsules in the absence of Cy5-PEG-cholesterol, capsules in solution with Cy5-PEG_{3500}-cholesterol, and capsules purified from this solution by centrifugation, washing, and resuspension in water. Values shown as mean ± SD, n = 3. B-D) CLSM image of APCN capsules functionalized with Cy5-PEG_{3500}-cholesterol: B) Cy5 channel, C) transmission channel, D) overlay. The depicted microcapsules were prepared with PtNPs in the inner phase. Scale bars = 200 µm.

Supporting Information

Supporting Information is available from the Wiley Online Library or from the author.

Acknowledgements

The authors thank Dr. Goran Vladisavljević (Loughborough University, UK) for introducing us to the Lego-inspired microfluidic device, for providing us with one, and for guiding us in setting it up in the labs. The project received funding from the Partnership for International Research and Education (PIRE) Bio-inspired Materials and Systems, supported by the U.S. National Science Foundation under (Grant No. OISE 1844463) and the Swiss National Science Foundation under (Grant No IZPIP0_177995). Moreover, this work benefitted from support from the Swiss National Science Foundation through the National Center of Competence in Research (NCCR) Bio-Inspired Materials (Grant No 51NF40-182881). Furthermore, this project has received funding from the European Union's Horizon 2020 research and innovation programme under the Marie Skłodowska-Curie grant agreement No 101032493 (AB) and funding from the Mac Robertson postgraduate travel scholarship awarded

in 2020 by the University of Glasgow and the University of Strathclyde (STRV).

Conflict of Interest

The authors declare no conflict of interest.

Data Availability Statement

The datasets generated and analyzed during the current study are available in the University of Strathclyde's Pure repository, https://doi.org/10.15129/873f0d6d-16b3-4fab-bc07-9a903bc04d8c.

Keywords

amphiphilic polymer conetworks, lego-inspired glass capillary microfluidic device, microcapsules, micro- and nanoreactors, microfluidic double emulsion

Received: January 23, 2024
Revised: March 9, 2024
Published online:

[1] S. S. Datta, A. Abbaspourrad, E. Amstad, J. Fan, S.-H. Kim, M. Romanowsky, H. C. Shum, B. Sun, A. S. Utada, M. Windbergs, S. Zhou, D. A. Weitz, *Adv. Mater.* **2014**, *26*, 2205.
[2] J.-W. Kim, S. H. Han, Y. H. Choi, W. M. Hamonangan, Y. Oh, S.-H. Kim, *Lab Chip.* **2022**, *22*, 2259.
[3] M. Duran, A. Serrano, A. Nikulin, J.-L. Dauvergne, L. Derzsi, E. Palomo del Barrio, *Mater. Des.* **2022**, *223*, 111230.
[4] P. W. Chen, R. M. Erb, A. R. Studart, *Langmuir.* **2012**, *28*, 144.
[5] Z. Liu, F. Fontana, A. Python, J. T. Hirvonen, H. A. Santos, *Small.* **2020**, *16*, 1904673.
[6] Y. Zheng, Z. Wu, L. Lin, X. Zheng, Y. Hou, J.-M. Lin, *Lab Chip.* **2021**, *21*, 4311.
[7] T. Y. Lee, T. M. Choi, T. S. Shim, R. A. M. Frijns, S.-H. Kim, *Lab Chip.* **2016**, *16*, 3415.
[8] S. Russell, N. Bruns, *Macromol. Rapid Commun.* **2023**, *44*, 2300120.
[9] G. Michielin, S. J. Maerkl, *Sci. Rep.* **2022**, *12*, 21391.
[10] J. Liu, H. Chen, X. Shi, S. Nawar, J. G. Werner, G. Huang, M. Ye, D. A. Weitz, A. A. Solovev, Y. Mei, *Environ. Sci.: Nano.* **2020**, *7*, 656.
[11] C. Nam, J. Yoon, S. A. Ryu, C.-H. Choi, H. Lee, *ACS Appl. Mater. Interfaces.* **2018**, *10*, 40366.
[12] D. G. Moore, T. A. Moser, P. A. Rühs, A. R. Studart, *Adv. Mater. Interfaces.* **2018**, *5*, 1800813.
[13] E. Loiseau, P. A. Rühs, A. Hauser, F. Niedermair, G. Albrecht, A. R. Studart, *Langmuir.* **2018**, *34*, 205.
[14] J. S. Sander, A. R. Studart, *Langmuir.* **2011**, *27*, 3301.
[15] C. S. Patrickios, T. K. Georgiou, *Curr. Opin. Colloid Interface Sci.* **2003**, *8*, 76.
[16] G. Erdodi, J. P. Kennedy, *Prog. Polym. Sci.* **2006**, *31*, 1.
[17] L. Mespouille, J. L. Hedrick, P. Dubois, *Soft Matter.* **2009**, *5*, 4878.
[18] A. Ramazani, A. Dabbaghi, F. Gouranlou, *Curr. Org. Chem.* **2018**, *22*, 362.
[19] C. S. Patrickios, in *Amphiphilic Polymer Co-networks: : Synthesis, Properties, Modelling and Applications*, (Ed: C. S. Patrickios,) The Royal Society of Chemistry, Cambridge, UK **2020**, Ch1.
[20] C. S. Patrickios, K. Matyjaszewski, *Polym. Int.* **2021**, *70*, 10.
[21] C. K. Varnava, C. S. Patrickios, *Polymer.* **2021**, *215*, 123322.
[22] K. Yamamoto, E. Ito, S. Fukaya, H. Takagi, *Macromolecules.* **2009**, *42*, 9561.
[23] K. Suevegh, A. Domjan, G. Vanko, B. Ivan, A. Vertes, *Macromolecules.* **1998**, *31*, 7770.
[24] J. Scherble, R. Thomann, B. Ivan, R. Mülhaupt, *J. Polym. Sci., Part B: Polym. Phys.* **2001**, *39*, 1429.
[25] A. Domján, G. Erdödi, M. Wilhelm, M. Neidhöfer, K. Landfester, B. Iván, H. W. Spiess, *Macromolecules.* **2003**, *36*, 9107.
[26] N. Bruns, J. Scherble, L. Hartmann, R. Thomann, B. Iván, R. Mülhaupt, J. C. Tiller, *Macromolecules.* **2005**, *38*, 2431.
[27] C. N. Walker, K. C. Bryson, R. C. Hayward, G. N. Tew, *ACS Nano.* **2014**, *8*, 12376.
[28] Y. Shi, H. Schmalz, S. Agarwal, *Polym. Chem.* **2015**, *6*, 6409.
[29] X. H. Zhang, K. Kyriakos, M. Rikkou-Kalourkoti, E. N. Kitiri, C. S. Patrickios, C. M. Papadakis, *Colloid. Polym. Sci.* **2016**, *294*, 1027.
[30] K. Yamamoto, E. Ito, Y. Mori, *Macromol. Symp.* **2019**, *385*, 1800181.
[31] T. Stumphauser, G. Kasza, A. Domján, A. Wacha, Z. Varga, Y. Thomann, R. Thomann, B. Pásztói, T. M. Trötschler, B. Kerscher, R. Mülhaupt, B. Iván, *Polymers.* **2020**, *12*, 2292.
[32] L. Benski, I. Viran, F. Katzenberg, J. C. Tiller, *Macromol. Chem. Phys.* **2021**, *222*, 2000292.
[33] S. A. Wilhelm, M. Maricanov, V. Brandt, F. Katzenberg, J. C. Tiller, *Polymer.* **2022**, *242*, 124582.
[34] D. E. Apostolides, C. S. Patrickios, T. Sakai, M. Guerre, G. Lopez, B. Améduri, V. Ladmiral, M. Simon, M. Gradzielski, D. Clemens, C. Krumm, J. C. Tiller, B. Ernould, J.-F. Gohy, *Macromolecules.* **2018**, *51*, 2476.
[35] D. E. Apostolides, C. S. Patrickios, M. Simon, M. Gradzielski, A. Blanazs, C. Mussault, A. Marcellan, N. Alexander, C. Wesdemiotis, *Polym. Chem.* **2023**, *14*, 201.
[36] C. Mugemana, P. Grysan, R. Dieden, D. Ruch, N. Bruns, P. Dubois, *Macromol. Chem. Phys.* **2020**, *221*, 1900432.
[37] C. Mugemana, G. Mertz, P. Grysan, R. Dieden, D. Ruch, *Macromol. Chem. Phys.* **2023**, *224*, 2200456.
[38] D. G. Tsalikis, M. Ciobanu, C. S. Patrickios, Y. Higuchi, *Macromolecules.* **2023**, *56*, 9299.
[39] S. Shamlou, J. P. Kennedy, R. P. Levy, *J. Biomed. Mater. Res.* **1997**, *35*, 157.
[40] F. E. Du Prez, E. J. Goethals, R. Schue, H. Qariouh, F. Schue, *Polym. Int.* **1998**, *46*, 117.
[41] J. Tobis, L. Boch, Y. Thomann, J. C. Tiller, *J. Membr. Sci.* **2011**, *372*, 219.
[42] H. Zhang, Y. Zhang, L. Li, S. Zhao, H. Ni, S. Cao, J. Wang, *Chem. Eng. Sci.* **2014**, *106*, 157.
[43] K. Schöller, S. Küpfer, L. Baumann, P. M. Hoyer, D. de Courten, R. M. Rossi, A. Vetushka, M. Wolf, N. Bruns, L. J. Scherer, *Adv. Funct. Mater.* **2014**, *24*, 5194.
[44] S. Ulrich, L. F. Boesel, N. Bruns, in *Amphiphilic Polymer Co-networks: Synthesis, Properties, Modelling and Applications*, (Ed: C. S. Patrickios), The Royal Society of Chemistry, Cambridge, UK **2020**, p. 331.
[45] J. P. Kennedy, G. Fenyvesi, R. P. Levy, K. S. Rosenthal, *Macromol. Symp.* **2001**, *172*, 56.
[46] Y. Yuan, A.-K. Zhang, J. Ling, L.-H. Yin, Y. Chen, G.-D. Fu, *Soft Matter.* **2013**, *9*, 6309.
[47] J. Xu, L. Zhang, Y. Zhang, T. Li, G. Huo, *J. Biomater. Sci., Polym. Ed.* **2014**, *25*, 121.
[48] A. K. S. Chandel, C. U. Kumar, S. K. Jewrajka, *ACS Appl. Mater. Interfaces.* **2016**, *8*, 3182.
[49] N. Bruns, J. C. Tiller, *Macromolecules.* **2006**, *39*, 4386.
[50] C.-S. Huang, K. Jakubowski, S. Ulrich, S. Yakunin, M. Clerc, C. Toncelli, R. M. Rossi, M. V. Kovalenko, L. F. Boesel, *Nano Energy.* **2020**, *76*, 105039.

[51] C.-S. Huang, S. Yakunin, J. Avaro, X. Kang, M. I. Bodnarchuk, M. Liebi, X. Sun, R. M. Rossi, M. V. Kovalenko, L. F. Boesel, *Adv. Energy Mater.* **2022**, *12*, 2200441.
[52] J. P. Kennedy, *J. Macromol. Sci., Pure Appl. Chem. A.* **1994**, *31*, 1771.
[53] R. Blezer, T. Lindhout, B. Keszler, J. P. Kennedy, *Polym. Bull. (Berlin).* **1995**, *34*, 101.
[54] D. Chen, J. P. Kennedy, M. M. Kory, D. L. Ely, *J. Biomed. Mater. Res.* **1989**, *23*, 1327.
[55] J. Kang, G. Erdodi, J. P. Kennedy, *J. Polym. Sci., Part A: Polym. Chem.* **2007**, *45*, 4276.
[56] H. Wang, C. Zhang, J. Wang, X. Feng, C. He, *ACS Sustainable Chem. Eng.* **2016**, *4*, 3803.
[57] S. Liu, M. Dong, Z. Zhang, G. Fu, *Polym. Adv. Technol.* **2017**, *28*, 1065.
[58] D. Park, B. Keszler, V. Galiatsatos, J. P. Kennedy, *J. Appl. Polym. Sci.* **1997**, *66*, 901.
[59] I. S. Isayeva, A. N. Gent, J. P. Kennedy, *J. Polym. Sci., Part A: Polym. Chem.* **2002**, *40*, 2075.
[60] J. Xu, D. A. Bohnsack, M. E. Mackay, K. L. Wooley, *J. Am. Chem. Soc.* **2007**, *129*, 506.
[61] M. Vamvakaki, C. S. Patrickios, *Soft Matter.* **2008**, *4*, 268.
[62] G. Guzman, T. Nugay, I. Nugay, N. Nugay, J. Kennedy, M. Cakmak, *Macromolecules.* **2015**, *48*, 6251.
[63] S. T. R. Velasquez, D. Jang, P. Jenkins, P. Liu, L. Yang, L. T. J. Korley, N. Bruns, *Adv. Funct. Mater.* **2022**, *32*, 2207317.
[64] P. C. Nicolson, J. Vogt, *Biomaterials.* **2001**, *22*, 3273.
[65] Z. Mutlu, S. Shams Es-haghi, M. Cakmak, *Adv. Healthcare Mater.* **2019**, *8*, 1801390.
[66] S. Diamanti, in *Amphiphilic Polymer Co-networks: Synthesis, Properties, Modelling and Applications*, (Ed: C. S. Patrickios), The Royal Society of Chemistry, **2020**, p. 0.
[67] G. Guzman, S. S. Es-haghi, T. Nugay, M. Cakmak, *Adv. Healthcare Mater.* **2017**, *6*, 1600775.
[68] B. Ivan, J. P. Kennedy, P. W. Mackey, *Polym. Prepr. (Am. Chem. Soc., Div. Polym. Chem.)*. **1990**, *31*, 215.
[69] B. Ivan, J. P. Kennedy, P. W. Mackey, *Polym. Prepr. (Am. Chem. Soc., Div. Polym. Chem.)* **1990**, *31*, 217.
[70] B. Iván, J. P. Kennedy, P. W. Mackey, *ACS Symp. Ser.* **1991**, *469*, 203.
[71] J. P. Kennedy, G. Fenyvesi, S. Na, B. Keszler, K. S. Rosenthal, *Des. Monomers Polym.* **2000**, *3*, 113.
[72] J. C. Tiller, C. Sprich, L. Hartmann, *J. Controlled Release.* **2005**, *103*, 355.
[73] B. Lu, M. D. Tarn, N. Pamme, T. K. Georgiou, *J. Mater. Chem. B.* **2015**, *3*, 4524.
[74] B. Lu, M. D. Tarn, N. Pamme, T. K. Georgiou, *J. Mater. Chem. B.* **2016**, *4*, 3086.
[75] B. Lu, M. D. Tarn, N. Pamme, T. K. Georgiou, *J. Polym. Sci., Part A: Polym. Chem.* **2018**, *56*, 59.
[76] I. S. Isayeva, B. T. Kasibhatla, K. S. Rosenthal, J. P. Kennedy, *Biomaterials.* **2003**, *24*, 3483.
[77] J. Kang, G. Erdodi, J. P. Kennedy, H. Chou, L. Lu, S. Grundfest-Broniatowski, *Macromol. Biosci.* **2010**, *10*, 369.
[78] N. Bruns, J. C. Tiller, *Nano Lett.* **2005**, *5*, 45.
[79] G. Savin, N. Bruns, Y. Thomann, J. C. Tiller, *Macromolecules.* **2005**, *38*, 7536.
[80] N. Bruns, W. Bannwarth, J. C. Tiller, *Biotechnol. Bioeng.* **2008**, *101*, 19.
[81] J. C. Tiller, C. Sprich, L. Hartmann, *J Control Release.* **2005**, *103*, 355.
[82] C.-S. Huang, X. Kang, R. M. Rossi, M. V. Kovalenko, X. Sun, H. Peng, L. F. Boesel, *J. Mater. Chem. A.* **2021**, *9*, 25974.
[83] M. Hanko, N. Bruns, J. C. Tiller, J. Heinze, *Anal. Bioanal. Chem.* **2006**, *386*, 1273.
[84] M. Hanko, N. Bruns, S. Rentmeister, J. C. Tiller, J. Heinze, *Anal. Chem.* **2006**, *78*, 6376.
[85] S. Ulrich, A. Osypova, G. Panzarasa, R. M. Rossi, N. Bruns, L. F. Boesel, *Macromol. Rapid Commun.* **2019**, *40*, 1900360.
[86] M. Rother, J. Barmettler, A. Reichmuth, J. V. Araujo, C. Rytka, O. Glaied, U. Pieles, N. Bruns, *Adv. Mater.* **2015**, *27*, 6620.
[87] S. Ulrich, A. Sadeghpour, R. M. Rossi, N. Bruns, L. F. Boesel, *Macromolecules.* **2018**, *51*, 5267.
[88] M. V. Bandulasena, G. T. Vladisavljević, B. Benyahia, *J. Colloid Interface Sci.* **2019**, *542*, 23.
[89] N. Leister, G. T. Vladisavljević, H. P. Karbstein, *J. Colloid Interface Sci.* **2022**, *611*, 451.
[90] E. Katifori, S. Alben, E. Cerda, D. R. Nelson, J. Dumais, *Proc. Natl. Acad. Sci. USA.* **2010**, *107*, 7635.
[91] A. Belluati, S. Jimaja, R. J. Chadwick, C. Glynn, M. Chami, D. Happel, C. Guo, H. Kolmar, N. Bruns, *Nat. Chem.* **2023**. https://doi.org/10.1038/s41557-023-01391-y
[92] D. G. Moore, J. V. A. Brignoli, P. A. Ruhs, A. R. Studart, *Langmuir.* **2017**, *33*, 9007.
[93] G. Nurumbetov, N. Ballard, S. A. F. Bon, *Polym Chem-Uk.* **2012**, *3*, 1043.
[94] W. Shi, J. E. Didier, D. E. Ingber, D. A. Weitz, *ACS Appl. Mater. Interfaces.* **2018**, *10*, 31865.
[95] W. Zhang, L. Qu, H. Pei, Z. Qin, J. Didier, Z. Wu, F. Bobe, D. E. Ingber, D. A. Weitz, *Small.* **2019**, *15*, 1903087.
[96] A. C. M. Kuo, in *Polymer Data Handbook*, (Ed: J. E. Mark), Oxford University Press, New York, USA **1999**, p. 411.
[97] I. Yildirim, P. Sungur, A. C. Crecelius-Vitz, T. Yildirim, D. Kalden, S. Hoeppener, M. Westerhausen, C. Weber, U. S. Schubert, *Polym. Chem.* **2017**, *8*, 6086.
[98] B. Aran, M. Sankır, E. Vargün, N. D. Sankır, A. Usanmaz, *J. Appl. Polym. Sci.* **2010**, *116*, 628.
[99] V. Maffeis, A. Belluati, I. Craciun, D. Wu, S. Novak, C.-A. Schoenenberger, C. G. Palivan, *Chem. Sci.* **2021**, *12*, 12274.
[100] M. E. Seitz, M. E. Wiseman, I. Hilker, J. Loos, M. Tian, J. Li, M. Goswami, V. M. Litvinov, S. Curtin, M. Bulters, *Polymer.* **2017**, *118*, 150.
[101] A. Belluati, I. Craciun, C. E. Meyer, S. Rigo, C. G. Palivan, *Curr. Opin. Biotechnol.* **2019**, *60*, 53.
[102] R. Serra-Maia, M. Bellier, S. Chastka, K. Tranhuu, A. Subowo, J. D. Rimstidt, P. M. Usov, A. J. Morris, F. M. Michel, *ACS Appl. Mater. Interfaces.* **2018**, *10*, 21224.
[103] P. George, D. H. Irvine, *Biochem. J.* **1952**, *52*, 511.
[104] C. Guo, R. J. Chadwick, A. Foulis, G. Bedendi, A. Lubskyy, K. J. Rodriguez, M. M. Pellizzoni, R. D. Milton, R. Beveridge, N. Bruns, *ChemBioChem.* **2022**, *23*, 202200197.
[105] I. Vlasova, *Molecules.* **2018**, *23*, 2561.
[106] D. Dębski, R. Smulik, J. Zielonka, B. Michałowski, M. Jakubowska, K. Dębowska, J. Adamus, A. Marcinek, B. Kalyanaraman, A. Sikora, *Free Radical Biol. Med.* **2016**, *95*, 323.
[107] A. Belluati, I. Craciun, J. Liu, C. G. Palivan, *Biomacromolecules.* **2018**, *19*, 4023.
[108] J. W. Swarts, R. C. Kolfschoten, M. C. A. A. Jansen, A. E. M. Janssen, R. M. Boom, *Chem. Eng. J.* **2010**, *162*, 301.
[109] R. Luo, K. Göpfrich, I. Platzman, J. P. Spatz, *Adv. Funct. Mater.* **2020**, *30*, 2003480.
[110] A. Belluati, I. Harley, I. Lieberwirth, N. Bruns, *Small* **2023**, *19*, 2303384.